Accepted Manuscript

IrO$_2$-Ta$_2$O$_5$|Ti electrodes prepared by electrodeposition from different Ir:Ta ratios for the degradation of polycyclic aromatic hydrocarbons

Rosa Alhelí Herrada, Gustavo Acosta-Santoyo, Selene Sepúlveda-Guzmán, Enric Brillas, Ignasi Sirés, Erika Bustos

Please cite this article as: Rosa.Alhelí. Herrada, G. Acosta-Santoyo, S. Sepúlveda-Guzmán, E. Brillas, I. Sirés, E. Bustos, IrO$_2$-Ta$_2$O$_5$|Ti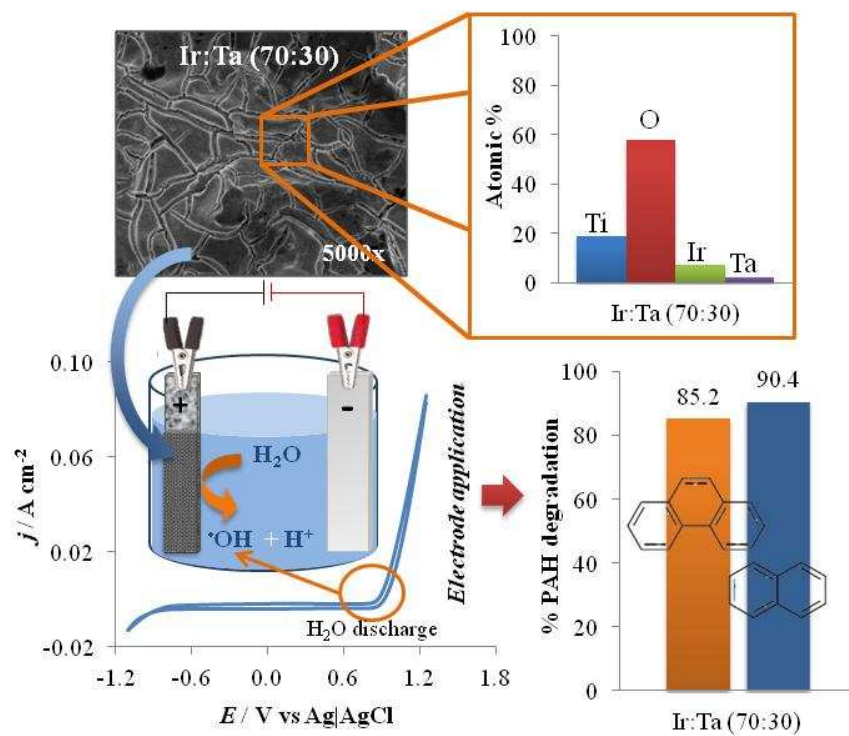 electrodes prepared by electrodeposition from different Ir:Ta ratios for the degradation of polycyclic aromatic hydrocarbons, *Electrochimica Acta* (2018), doi: 10.1016/j.electacta.2018.01.056.

This is a PDF file of an unedited manuscript that has been accepted for publication. As a service to our customers we are providing this early version of the manuscript. The manuscript will undergo copyediting, typesetting, and review of the resulting proof before it is published in its final form. Please note that during the production process errors may be discovered which could affect the content, and all legal disclaimers that apply to the journal pertain.
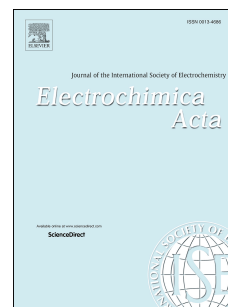
GRAHICAL ABSTRACT

1   IrO$_2$-Ta$_2$O$_5$|Ti electrodes prepared by electrodeposition from different

2   Ir:Ta ratios for the degradation of polycyclic aromatic hydrocarbons

3   Rosa Alhelí Herrada [a,b], Gustavo Acosta-Santoyo [a], Selene Sepúlveda-Guzmán [c],

4   Enric Brillas [b,#], Ignasi Sirés [b,*,#], Erika Bustos [a,**,#]

5   [a] *Centro de Investigación y Desarrollo Tecnológico en Electroquímica, S.C. Parque Tecnológico*

6   *Querétaro, Sanfandila, Pedro Escobedo, 76703 Querétaro, Mexico*

7   [b] *Laboratori d'Electroquímica dels Materials i del Medi Ambient, Departament de Química Física,*

8   *Facultat de Química, Universitat de Barcelona, Martí i Franquès 1-11, 08028 Barcelona, Spain*

9   [c] *Universidad Autónoma de Nuevo León, UANL, Facultad de Ingeniería Mecánica y Eléctrica,*

10   *FIME, Ave. Pedro de Alba s/n, Ciudad Universitaria, C.P.66455 San Nicolás de los Garza, N.L.,*

11   *Mexico*

13   * Corresponding author: Tel.: +34 934039240; fax: +34 934021231.

14   E-mail address: i.sires@ub.edu (I. Sirés)

15   ** Corresponding author: Tel.: +52 442 2 11 60 59; fax: +52 442 2 11 60 01.

16   E-mail address: ebustos@cideteq.mx (E. Bustos)

17   [#]Active ISE member

Abstract

This work investigates the feasibility of producing IrO_2-Ta_2O_5|Ti electrodes by electrodeposition. Using precursor solutions with Ir:Ta molar ratios from 0:100 to 100:0, followed by thermal treatment, the goal was to find the optimal composition for enhancing the formation of hydroxyl radicals and providing long service lives. Scanning electron microscopy (SEM), coupled with energy dispersive X-ray spectroscopy (EDX), revealed that the production of homogeneous coatings with a good surface coverage and absence of agglomerates was only possible for electrodes with 70% or 100% Ir. The potential for O_2 evolution was similar for all the electrodes containing Ir, at about 0.90 V vs Ag|AgCl. However, the ability to produce M($^\bullet$OH) clearly increased with increasing Ir in the Ir:Ta ratios (100:0 > 70:30 > 30:70 > 0:100). This observation was confirmed by the transformation of coumarin to 7-hydroxycoumarin as determined by spectroscopic and chromatographic techniques after treatment. Once manufactured and characterized, the electrodes were tested, as anodes, for the electro-oxidation of polycyclic aromatic hydrocarbons in aqueous solutions at natural pH (i.e., without pH adjustment). The anodes prepared from 70:30 and 100:0 ratios produced the fastest and highest removal rates, reaching 86% and 93% for phenanthrene and naphthalene, respectively, after 120 min at 50 mA. This was accompanied by a high degree of mineralization, as the result of direct and M($^\bullet$OH)-mediated oxidation, with some refractory intermediates remaining in the final solutions. The interaction between IrO_2 and Ta_2O_5 oxides appeared to be important. The 100:0 anode provided high electrocatalytic effectiveness, whereas the anode with the 70:30 ratio provided improved long-term stability, as confirmed by its service life of about 93 h.

1. Introduction

Interest in electrochemical science and technology is growing worldwide, in large part because of their ability to devise new systems that ensure significant societal progress as they can lower negative environmental impacts when compared to old and well established processes [1]. The electrochemical technologies for water treatment are a clear example of this since they combine high efficiency, with low resource consumption, by using the electron as a 'clean reagent' [2]. Within this field, the so-called electrochemical advanced oxidation processes (EAOPs) have proven most successful for the degradation of organic pollutants. In many cases it is possible to achieve the complete detoxification of water streams with their use [3,4]. This outstanding performance, when coupled with reduced energy consumption in properly designed cell configurations and the appropriate electrode materials are chosen, follows from their ability to produce reactive oxygen species (ROS), like the hydroxyl radical ($^\bullet$OH), in-situ and in controlled ways with the correct modulation of the electrolytic conditions.

Boron-doped diamond (BDD) is considered the most powerful anode for removing organic contaminants from aqueous solutions by the production of quasi-free hydroxyl radicals through the oxidation of water at a high electrode potential following the Reaction (1) [5]:

$$M + H_2O \rightarrow M(^\bullet OH) + H^+ + e^- \tag{1}$$

Despite its potential, BDD has several significant drawbacks that hamper its wider implementation on a large scale. It is expensive and very few substrate materials can be used to support stable thin films of BDD for use as anode. Additionally, the electrodes are brittle or exhibit poor electrical conductivity meaning that they are not acceptable for large scale industrial or municipal applications [6].

The need to reduce the cost of electrode materials has led to the synthesis of photoanodes, which allow the treatment of pollutants by an EAOP called photoelectrocatalysis [7], where artificial UV light, or natural sunlight, stimulate the production of hydroxyl radicals on the surface

3

66 of the photocatalysts. Alternatively, non photoactive but highly oxidizing dimensionally stable

67 anodes suitable for O_2 or Cl_2 evolution have been manufactured by preparing mixtures of different

68 metal oxides [8]. These anodes employ an electrocatalytic oxide film, usually based on RuO_2 or

69 IrO_2, deposited on a suitable metal substrate like titanium (Ti). These anodes exhibit appealing

70 technological properties including long-term mechanical and chemical stability and high catalytic

71 activity [2]. Aiming to increase the film stability, other oxides (e.g., TiO_2, SnO_2, Ta_2O_5) are added,

72 thus obtaining a greater corrosion resistance and diminishing the amount of the catalytic oxide

73 needed which, in turn, minimizes production costs [9,10]. Single- and mixed-metal oxides are then

74 employed for the electro-oxidation (EO) of organic pollutants. EO is the paradigm of sustainability

75 among the EAOPs, since no addition of processing chemicals is needed. Its operational simplicity,

76 combined with high effectiveness, has led to wider implementation when compared to other

77 EAOPs. In EO, adsorbed $M(^{\bullet}OH)$ are produced by Reaction (1), with these being further

78 transformed into a less powerful oxidant like chemisorbed "superoxide" MO [11]. Different kinds

79 of dimensionally stable anodes have been used for the EO treatment of a large variety of organic

80 molecules [12-21]. In the presence of Cl^- ions, the complexity of EO increases significantly due to

81 the oxidation of this anion to active chlorine according to Reaction (2), (a process exploited in the

82 chlor-alkali industry) [6]:

83 $2\,Cl^- \rightarrow Cl_{2(aq)} + 2\,e^-$ (2)

84 ClO_2, $ClO^-/HClO$, ClO_2^-, ClO_3^- and ClO_4^- can also be formed, depending on the operational

85 conditions including exposure time, temperature, electrode materials and hydrodynamic conditions

86 [22].

87 Owing to their low cost, oxide-based anodes have also found use as a counter electrode in

88 Fenton-based EAOPs including electro-Fenton [20,23-27], electro-Fenton-like [28] and UVA or

89 solar photoelectro-Fenton [20]. In these processes the degradation of the pollutants is mainly guided

90 by the action of free $^{\bullet}OH$ radicals generated in the bulk.

4

91   In spite of the reported superiority of BDD over other potential anodes, some exceptions have

92   been reported. For example, Coria et al. [29] found a greater removal of total organic carbon (TOC)

93   using an IrO_2-based anode as compared to BDD during the treatment of naproxen by EO. This

94   result was attributed to higher adsorption of organics on the anode surface. Results like these, when

95   combined with improved industrial success of mixed metal oxides [30] and the higher corrosion

96   resistance and longer service life of IrO_2-based anodes as compared to RuO_2-based ones [31-33],

97   justify the interest in the optimization of the synthesis of IrO_2-based dimensionally stable anodes.

98   Specifically, those developed as a metal-oxide mixture, with Ta_2O_5 as the stabilizer, seem the most

99   interesting. These mixed-oxide anodes are more electrochemically stable and exhibit enhanced

100   service life from the coating [34] than pure IrO_2-based anodes.

101   In the modern world, the availability of clean water has become increasingly problematic due

102   to both natural causes and human activity [35]. One significant problem is the presence of

103   polycyclic aromatic hydrocarbons (PAHs), which can be produced during the incomplete

104   combustion of organic materials including coal, oil, gas, wood, garbage, and tobacco. PAHs, due to

105   inefficient removal processes, have been found widely in municipal wastewater and industrial

106   effluents [36]. As a consequence of their hydrophobic nature, PAHs tend to become strongly

107   adsorbed in sediments and aquatic organisms, as well as on the surface of particulates including

108   micro-plastics [37], whose presence in water is also a very critical issue [38]. PAHs are included in

109   a group of organic pollutants causing significant concern within the European Union [39], as they

110   are suspected of being mutagens, carcinogens and endocrine disruptors [40].

111   Several authors have reported the electrochemical treatment of various PAHs with different

112   types of mixed metal oxides [41-43]. Our teams have recently shown the feasibility of PAHs

113   removal by EO with IrO_2-based anodes synthesized using different techniques [44]. Classical

114   synthesis routes have included thermal decomposition and the sol-gel 'Pechini' method [28].

115   Reactive sputtering [45] and physical vapor deposition [46] are other existing alternatives. This

5

116 work addresses the synthesis of IrO_2-Ta_2O_5-coated Ti-electrodes by electrodeposition using four

117 different Ir:Ta ratios, to determine the optimal composition to stimulate the maximum concentration

118 of hydroxyl radicals to be available for treatment. All the electrodes were characterized by scanning

119 electron microscopy (SEM) coupled with energy dispersive X-ray spectroscopy (EDX), cyclic

120 voltammetry (CV) and accelerated life testing. During EO testing, the production of $M(^{\bullet}OH)$ was

121 monitored using either UV/vis spectrophotometry or liquid chromatography with fluorescence

122 detection. The oxidation power of these electrodes was verified by using them as anodes in the EO

123 treatment of synthetic aqueous solutions containing naphthalene or phenanthrene, monitoring the

124 concentration decay by high performance liquid chromatography (HPLC) and their mineralization

125 from the analysis of TOC abatement.

126 **2. Materials and methods**

127 *2.1. Electrode manufacture*

128 The precursor solutions were prepared using H_2IrCl_6 [31-34] and $TaCl_5$ [47], both purchased

129 from Strem Chemicals ($\geq$ 99.9% purity). They were then dissolved in HCl [44] and isopropanol

130 [34,44], respectively, under vigorous stirring. Four different test precursor solutions were further

131 prepared to be used in the coating process by mixing the appropriate amount of prepared metal

132 solutions to obtain Ir:Ta molar ratios of 100:0, 70:30, 30:70, and 0:100. Before electrodeposition,

133 the Ti-plates (each 5.0 mm $\times$ 15.0 mm $\times$ 1.0 mm) that were to be used as substrates were pretreated

134 by sandblasting [34,44], etching in a 40% oxalic acid solution for 20 min [31,44], and finally rinsed

135 with deionized water and dried. Electrochemical deposition was performed at a constant current

136 density of 14 mA cm^{-2} for 20 min under constant stirring at 825 rpm [44]. Once the coated Ti-

137 electrodes were prepared, the coatings were transformed into metal oxides using a 2-step thermal

138 decomposition procedure: heating at 523 K for 10 min, followed by heating to 723 K and holding

139 for 1 h [34,44]. Three electrodes, at each of the four coatings compositions, were prepared.

140 *2.2. Electrode characterization*

141   Microstructural analysis, to study the morphology of the deposits, was performed by SEM-

142 EDX using a Jeol JSM6500 microscope, operating at 15 kV. Surface distribution of Ir and Ta was

143 performed in the SEM using the Oxford Inca 300 EDX analyzer.

144   Electrochemical characterizations were made using cyclic voltammetry in a conventional three

145 electrode glass cell. Each of the various test IrO_2-Ta_2O_5|Ti electrodes was placed as the working

146 electrode (0.75 cm^2), with a platinum (Pt) wire (BASi) and an Ag|AgCl (3M KCl, BASi) used as

147 counter and reference electrodes, respectively, in the cell. All experiments were performed at 298 K

148 with 10 mL of 0.5 M H_2SO_4 (J. T. Baker, 98%) as supporting electrolyte and employing a

149 Bioanalytical Systems BAS-Epsilon™ potentiostat. Before the electrochemical tests, O_2 was purged

150 from the test cell by bubbling ultrapure nitrogen (Praxair, grade 5.0) through the electrolyte for at

151 least 20 min, and this gas continuously flowed over the solution during the measurement cycles. In

152 all the cyclic voltammograms shown in this work, the active area of each coated Ti-electrode has

153 been considered, as previously described [44]. For each of the different working electrode

154 compositions the tests were performed in triplicate.

155   The service life of each of the various IrO_2-Ta_2O_5|Ti coated electrodes was evaluated according

156 to the methodology reported in NACE TM0108 [48]. A two-electrode electrochemical cell was

157 employed, placing the coated electrodes as the working electrode (0.75 cm^2) and an uncoated Ti-

158 plate as a counter electrode (3.5 cm^2). These experiments were performed at 298 K with 70 mL of 1

159 M H_2SO_4 as supporting electrolyte using a constant current of 3.18 A (supplied by an EZ Digital

160 model GP-4303DU DC power supply), and with constant stirring at 825 rpm. As required in the

161 NACE TM0108 protocol, these tests were run until an increase of 30% was observed in the inter-

162 electrode potential difference compared to the initial value.

163   The production of hydroxyl radicals was evaluated from tests monitoring the transformation of

164 coumarin to 7-hydroxycoumarin [49]. For this, several electrolytic tests were performed using a

165 two-electrode electrochemical glass cell equipped with an anode, using one of each of the

166 compositional variation IrO_2-Ta_2O_5|Ti electrodes (0.75 cm^2), and a Pt-wire as the cathode. Solutions

167 of 10 mL of 0.3 mM coumarin (Sigma-Aldrich, 99%) in 0.5 M H_2SO_4 were electrolyzed at room

168 temperature and 50 mA under constant stirring. Samples were withdrawn at selected time periods to

169 monitor changes in the concentration of coumarin. Testing by UV/vis spectroscopy, on a Shimadzu

170 UV-1800 UV-Vis spectrophotometer within the range between 200 and 800 nm, was used during

171 these characterizations. For the same samples, the accumulation of 7-hydroxycoumarin was

172 assessed by HPLC using a Shimadzu LC-10ADVP chromatograph equipped with a Thermo

173 Electron Hypersil ODS (5 μm, 150 mm × 3 mm) column coupled to a Shimadzu RF-10AXL

174 fluorescence detector. An acetonitrile:water (60:40, v/v) mixture was used as a mobile phase to

175 elute the samples at a flow rate of 0.5 mL min^{-1}, with excitation and emission wavelengths of 325

176 nm and 400 nm, respectively. A 7-hydroxycoumarin analytical standard from Sigma-Aldrich was

177 used for quantification.

178 *2.3. Electrochemical degradation of hydrocarbons*

179 Bulk electrolyses for the performance evaluation of the manufactured electrodes to degrade

180 PAHs, such as phenanthrene and naphthalene, were made in a two-electrode electrochemical cell,

181 using the various IrO_2-Ta_2O_5|Ti electrodes (0.75 cm^2) and a Pt-plate as the anode and cathode.

182 Solutions of 50 mL containing either 2 μM phenanthrene (from Acros Organics, 97%) or 2 μM

183 naphthalene (from Alfa Aesar, 99%) in 0.05 M Na_2SO_4 at natural pH (i.e., without pH adjustment)

184 were treated at room temperature under a constant current of 50 mA and with constant stirring. To

185 investigate the decay kinetics of each pollutant, samples were withdrawn at selected times for 120

186 min and analyzed using a Waters 600 liquid chromatograph fitted with a BDS Hypersil C18 6 μm,

187 250 mm × 4.6 mm, column at 35 ℃ and coupled to a Waters 996 photodiode array detector set at λ

188 of 254 nm. These measurements were made by injecting 20 μL aliquots into the chromatograph

189 using a 60:40 (v/v) acetonitrile/water mixture at 1.3 mL min^{-1} as mobile phase. Peaks at 7.7 and

190   13.7 min were found for naphthalene and phenanthrene, respectively. Organic solvents and other

191   chemicals were of HPLC or analytical grade from Sigma-Aldrich and Panreac. All the solutions

192   were prepared using ultrapure water from a Millipore Milli-Q system (resistivity >18 MΩ cm).

193   To assess the mineralization ability of the anodes, the TOC content was monitored during the

194   treatment of 50 mL of 25 mg·L^{-1} TOC (0.19) naphthalene in 0.05 M Na_2SO_4, at room temperature

195   and 50 mA under constant stirring of 825 rpm (with natural pH), using the same experimental setup

196   mentioned and employed above. Samples were measured on a Shimadzu VCSN TOC analyzer,

197   after filtration with 0.45 µm PTFE filters (Whatman) over a 360 min test cycles. The results were

198   obtained with ±1% accuracy. The following reaction for total mineralization of naphthalene was

199   assumed:

200   $C_{10}H_8 + 20\,H_2O \rightarrow 10\,CO_2 + 48\,H^+ + 48\,e^-$ (3)
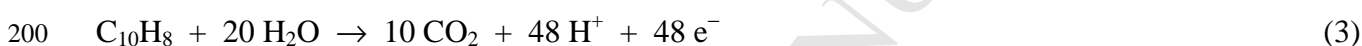
201   The mineralization current efficiency (MCE) values were estimated as follows [20]:

202   $\% \text{ MCE } = \dfrac{n\,F\,V\,\triangle(\text{TOC})_{\text{exp}}}{4.32 \times 10^7\,m\,I\,t} \times 100$ (4)

203   where $n = 48$ is the number of electrons for the mineralization, $m = 10$ is the number of carbon

204   atoms of naphthalene, and all the other parameters have been defined elsewhere [20].

205   **3. Results and discussion**

206   *3.1. Microstructural and electrochemical characterization*

207   Fig. 1A (at 2000x) and 1B (at 5000x) shows the surface morphologies of the four different

208   IrO_2-Ta_2O_5 coating layers found on the Ti-substrates after electrodeposition and heat cycling. In the

209   coatings prepared using Ir:Ta ratios of 100:0 and 70:30, it is possible to observe the cobblestone

210   morphology that is typical from this kind of mixed metal oxides manufactured at high temperature,

211   and please note its enhanced prominence in 70:30 coating. However, their surface appearance did

212   not exactly match a dried-mud cracked coating (i.e., mud-like islands surrounded by cracks) usually

9

213 observed after thermal decomposition at ≥ 450 ºC [50]. The distribution of cracks (see red arrows)

214 was not uniform over the entire surface as some areas were relatively flat and smooth. This may be

215 attributed to the particular distribution of Ir and Ta on the surface during the electrodeposition step.

216 Distributions using this method are clearly different from those resulting from a conventional

217 painting process or by immersion of the Ti-plate into a precursor solution. As a result, the fast

218 volatilization of solvents along with the high stress induced from anisotropic thermal expansion

219 (different expansion coefficients of Ti and coating) seem to be substantially minimized with the

220 electrochemical deposition treatment. This yields a more compact coating with no cracks connected

221 over long distances, eventually reducing the possibility of coating peeling-off. In contrast, in the

222 coatings prepared from predominately Ta ratios (30:70 and 0:100), whose microstructure when

223 viewed at higher magnification is shown in Fig. 1B, the presence of aggregates with greater

224 roughness can be identified (as indicated by green arrows). This suggests poor mixing of metal

225 oxides during electrodeposition, which would likely be detrimental for further application. A poor

226 distribution of Ta_2O_5 will lead to poor separation between the substrate and the IrO_2 catalytic layer,

227 promoting the passivation of the Ti-base metal. The presence of these kinds of agglomerates has

228 also been reported for layers formed using non-electrochemical procedures [34].

229   Fig. 2 shows the atomic percentages of Ti, Ir, Ta and oxygen determined by EDX for the four

230 different IrO_2-Ta_2O_5|Ti electrodes under study. No chloride, which could have been sourced from

231 the solutions used for the electrodeposition, was detected. The relative content of titanium and

232 oxygen is similar for the electrodes prepared from solutions at 100:0, 70:30 and 30:70 ratios, and

233 the proportion of Ir and Ta changes (as expected) from one to another. Importantly, the proportions

234 are in quite good agreement with the Ir:Ta molar ratios employed in each precursor solution. The

235 consistency of the resulting mixed metal oxide compositions suggested the absence of segregation,

236 a very positive feature that also occurs when using sol-gel preparation methods like Pechini´s [31].

237 In the coating prepared using only the Ta-containing precursor, the amount of titanium measured

was higher than expected and that of Ta was too low, a result suggesting that without Ir the deposition of Ta is neither homogeneous nor quantitative, leading to a partially uncoated Ti-substrate. Therefore, this low quality electrode might well be expected to perform worse than the others.

Fig. 3 presents the cyclic voltammograms recorded from test employing the four IrO_2-Ta_2O_5|Ti electrodes in 0.5 M H_2SO_4 at room temperature and a scan rate of 50 mV s^{-1}. The response for an uncoated Ti-substrate is not included but has been reported in earlier reports [44]. In this earlier study, no current steps were noted until a steep increase appeared in the anode potential vs Ag|AgCl at 0.05-0.10 V, which can be expected due to the low oxidation power of pure Ti-anodes. On the other hand, here it is possible to observe that for the three electrodes modified with IrO_2, the O_2 gas evolution occurred at a potential close to 0.90 V. According to Reaction (1), adsorbed hydroxyl radicals (M($^\bullet$OH)) should be generated as a first step, prior to gas evolution, and hence, their existence is investigated below. In addition, it can be seen that the increase in IrO_2 content in the coating, upon use of a higher initial Ir:Ta molar ratio from 30:70 to 100:0, enhances the response of the dimensionally stable anode, as deduced from the gradually greater current measured at a given potential over the oxygen evolution reaction (OER) region. Conversely, the electrochemical response of the electrode prepared with only Ta in the precursor solution (0:100 ratio) was much less significant using the same analytical sensitivity threshold. Thus, it can be concluded that Ta_2O_5 does not perform well as an electrocatalytic oxide for hydroxyl radical formation, but, rather it serves as an interlayer to promote coating adhesion and corrosion resistance for long term use in anodic electrodes [34,44,47].

3.2. Production of hydroxyl radicals

The treatment of 10 mL of a 0.3 mM coumarin solution in 0.5 M H_2SO_4 by EO with an IrO_2-Ta_2O_5|Ti anode and a Pt cathode at 50 mA allowed us to study the formation of M($^\bullet$OH) in two complementary ways. First, the decay of the coumarin content and second the generation of 7-

11

263 hydroxycoumarin formed upon hydroxylation of coumarin. Decay of coumarin was tracked by

264 UV/vis spectrophotometry over 180 min test cycles for the various anode materials. As observed in

265 Fig. 4, the anode without Ir (i.e., Ir:Ta ratio of 0:100) showed no decay of the coumarin absorbance,

266 due to a lack of electrode catalytic response (Fig. 3). In contrast, all the anodes containing Ir showed

267 decrease in coumarin content during the tests compared with the coumarin spectrum at time zero. A

268 greater rate of decay was observed as the Ir content in the precursor solution increased from 30% to

269 100%, confirming the catalytic ability of IrO_2. In particular, significant decays were found using the

270 70:30 and 100:0 ratios, which allows inferring a progressively larger production of M($^\bullet$OH),

271 although a more direct proof of hydroxyl radical generation is needed. For this, the samples

272 collected at the same electrolysis times were simultaneously analyzed, by HPLC coupled to

273 fluorescence detection, aiming to confirm and quantify the 7-hydroxycoumarin formed upon

274 hydroxylation of coumarin.

275   Fig. 5 presents the time variation of the 7-hydroxycoumarin concentration under each test

276 condition. The profiles confirm that as the the Ir:Ta molar ratio in the precursor solution increased

277 from 0:100 to 100:0, higher production of M($^\bullet$OH) was achieved. This is consistent with the

278 inactivity of pure Ta_2O_5 coatings as well as with the superior electrocatalytic power of layers with a

279 high content of IrO_2 (> 30%). Note that, as an additional proof of the formation of M($^\bullet$OH) in these

280 types of electrodes, in a previous work we reported the electron paramagnetic resonance (EPR)

281 analysis [44]. At this stage, the real performance of these IrO_2-Ta_2O_5|Ti electrodes as potential

282 anodes in typical treatment scenarios for the electro-oxidation of organic pollutants was studied.

283 *3.3. Electro-oxidation of aqueous solutions of PAHs*

284   The oxidation power of the four IrO_2-Ta_2O_5|Ti electrodes for degrading toxic organic pollutants

285 was tested in triplicate. Independent EO treatments of 50 mL of solutions containing ~ 2 μM of

286 each hydrocarbon in 0.05 M Na_2SO_4, at natural pH and room temperature by applying 50 mA were

287 carried out. Phenanthrene (see Fig 6A) and naphthalene (see Fig. 6B) were chosen as model PAHs,

12

since serious concerns have arisen about their presence in the environment. The decline in their concentration, as a function of electrolysis time, is shown in the two figures. Note, too, that the anode prepared without Ir (0:100 ratio) was able to remove 65%-70% phenanthrene (Fig. 6A) and 79%-84% naphthalene (Fig. 6B) at 120 min, despite its poor ability to produce M($^\bullet$OH) (Fig. 4 and 5). This suggests the occurrence of direct anodic oxidation of both hydrocarbons at the $Ta_2O_5|Ti$ anodic surface. Direct oxidation of organic aromatic compounds upon adsorption on the anode surface has been suggested before, in phenol treatments for example [6]. Within the framework of PAHs oxidation, it is known that multiple bonds with angular arenes are particularly prone to electron loss. Phenanthrene is a typical substrate with such activated bonds [51] and thus, it can be gradually transformed into several intermediates. Anthracene, whose structure is similar to that of phenanthrene and naphthalene, has also been reported to become oxidized directly at the anode, yielding a radical carbocation that, in the presence of water, is not dimerized but hydrolyzed and further oxidized to anthraquinone [52].

As seen in Fig. 6A and 6B, all the electrode coatings containing Ir promoted a faster and greater degradation of both PAHs, in agreement with the induced formation of M($^\bullet$OH) in the presence of IrO_2. In the case of phenanthrene, the anode at the 70:30 ratio outperformed the others, reaching the limit of quantification (LOQ) of 0.3 μM at 120 min, which accounts for > 86% removal. For naphthalene, the anodes prepared with 100:0 and 70:30 ratios performed similarly and both reached the naphthalene LOQ, of 0.15 μM, and greater than 93% removal during testing. Taken together, the decay of contaminants with and without Ir, one can conclude that the IrO_2-$Ta_2O_5|Ti$ anodes degrade phenanthrene and naphthalene by combined direct and M($^\bullet$OH)-mediated oxidation processes. None of the concentration abatements can be associated to pseudo-first-order reaction kinetics which would have been expected for reactions between the organic pollutant and a constant concentration of M($^\bullet$OH) [20,29]. This fact further reinforces the idea of a simultaneous action of direct and indirect oxidation processes, whose contribution is time-dependent.

13

313   The ability of the four electrodes to completely destroy solution TOC was also assessed. Fig.

314   7A depicts the TOC abatement over time during the EO of 50 mL of a 25 mg·L^{-1} (0.19 mM)

315   naphthalene solution in 0.05 M Na$_2$SO$_4$ at natural pH by applying 50 mA. The anode with no IrO$_2$

316   exhibited a certain ability to transform the organic carbon to CO$_2$, reaching 56% mineralization at

317   360 min. The oxidation power of the anodes containing Ir was again evident as mineralization

318   reached 74% TOC removal (i.e., final TOC content of 6.5 mg L^{-1} TOC). At times less than 2 h, the

319   anodes prepared with only Ir and at Ir:Ta ratio 70:30 behaved better than the 30:70 material, as

320   expected due to their greater ability to form M($^{\bullet}$OH). However, no substantial differences were

321   observed between the three types of electrodes at the end of the electrolysis, This observation can

322   be explained by the generation of highly refractory intermediates, like carboxylic acids, that cannot

323   be easily degraded by M($^{\bullet}$OH) [3]. The presence of this type of stable compound was confirmed by

324   mineralization current efficiency profiles calculated from Eq. (4). As can be observed in Fig. 7B,

325   which charts MCE vs. time, the efficiency was highest during the early stages of the treatment tests,

326   reaching 8-10%, but it progressively decreased, as a result of the lower organic load and its higher

327   refractory nature, ending in values as low as ~ 3%.

328   *3.4. Service life testing*

329   From previous sections, it is clear that the presence of IrO$_2$ in the coatings is crucial to make

330   degradation occur more rapidly, and to a greater extent. We noted that the improvement found in

331   the performance by anodes coated with precursor solutions containing 70% and 100% Ir was

332   minimal. A final comparison between them would be determined by coating stability for extended

333   use. To study if any life-use differences existed between them, their service life was determined by

334   applying the NACE TM0108 standard service life procedure (see experimental section). In these

335   tests, a stable potential was initially observed, but a steep rise in potential was recorded once the

336   resistance of the anode increased dramatically, causing its failure. Increasing electrical resistance

337   can be attributed to the detachment (i.e., peeling-off) of the IrO$_2$, Ta$_2$O$_5$ or IrO$_2$-Ta$_2$O$_5$ coating from

14

338 the Ti-substrate [31]. In contrast to studies described above, a very remarkable superiority of the

339 electrode prepared with a 70:30 ratio can be easily seen in Fig. 8. It performed for nearly 93 h

340 before failure while each of the other three materials failed in less than 2 h. This electrode offers

341 advantage from the differing performance characteristics of the two metal oxides. Its relatively high

342 concentration of IrO_2 ensures significant production of M($^\bullet$OH), while the moderate quantity of

343 Ta_2O_5 provides coating stability against corrosion. The absence of this oxide in the electrode

344 prepared with 100% Ir causes a dramatic decay of its performance upon prolonged electrolysis.

345   Many researchers have studied the service lifetime of IrO_2-Ta_2O_5|Ti anodes under galvanostatic

346 conditions in 1 M H_2SO_4 over the potential region corresponding to the OER. Huang, et al. [50]

347 have recently prepared compositionally similar anodes by thermal treatment, reporting a service

348 lifetime between 70 and 110 h. Results presented here agree with those in Comninellis et al. [9],

349 who prepared IrO_2-Ta_2O_5|Ti electrodes by thermal decomposition at 550 ºC over a wide range of

350 compositions from 10 to 100 mol.% Ir. They reported maximum electroactivity, along with the

351 greatest electrode service life, for the electrodes containing 70% Ir.

352 **4. Conclusions**

353   IrO_2-Ta_2O_5|Ti electrodes have been successfully prepared by electrodeposition using precursor

354 solutions containing four different Ir:Ta molar ratios, followed by a two step thermal treatment. The

355 coated electrodes were then used as working electrodes in tests for the degradation of PAHs. The

356 electrodes prepared with an Ir:Ta ratio of 70:30 were found to be superior during testing. This

357 compositional ratio produced homogenous coatings showing good coverage and minimal

358 segregation. They displayed the longest service life (about 93 as compared to all the other

359 compositional electrodes with Ir content of 0%, 30%, and 100%. The ability of such an electrode to

360 generate M($^\bullet$OH) was confirmed by the gradual transformation of coumarin into 7-

361 hydroxycoumarin during testing. Its applicability to EO treatment of organic pollutants was tested

15

362 by treating aqueous solutions of phenanthrene and naphthalene, at natural pH and low current.

363 Removal of more than 86% and 93% (respectively) of these contaminates was observed after 120

364 min. A large degree of mineralization was also attained after 360 min, although the anode was

365 unable to degrade some highly refractory intermediates. The oxidation power of the electrodes

366 prepared from precursor solutions with 30% and 100% Ir provided similar degradation, but their

367 service life was found to be below 2 h. The electrode coated with only a Ta-containing precursor

368 exhibited limited catalytic power but it did remove some of the pollutants, likely by a direct anodic

369 oxidation of PAHs.

Acknowledgments

References

380 [1] S. Bebelis, K. Bouzek, A. Cornell, M.G.S. Ferreira, G.H. Kelsall, F. Lapicque, C. Ponce de

381 León, M.A. Rodrigo, F.C. Walsh, Highlights during the development of electrochemical

382 engineering, Chem. Eng. Res. Design 91 (2013) 1998-2020.

383 [2] Y. Feng, L. Yang, J. Liu, B.E. Logan, Electrochemical technologies for wastewater treatment

384 and resource reclamation, Environ. Sci.: Water Res. 2 (2016) 800-831.

385 [3] I. Sirés, E. Brillas, M.A. Oturan, M.A. Rodrigo, M. Panizza, Electrochemical advanced

386   oxidation processes: today and tomorrow. A review, Environ. Sci. Pollut. Res. 21 (2014)

387   8336-8367.

388 [4] C.A. Martínez-Huitle, M.A. Rodrigo, I. Sirés, O. Scialdone, Single and coupled

389   electrochemical processes and reactors for the abatement of organic water pollutants: A

390   critical review, Chem. Rev. 115 (2015) 13362-13407.

391 [5] A. Kapałka, G. Fóti, C. Comninellis, The importance of electrode material in environmental

392   electrochemistry. Formation and reactivity of free hydroxyl radicals on boron-doped diamond

393   electrodes, Electrochim. Acta 54 (2009) 2018-2023.

394 [6] M. Panizza, G. Cerisola, Direct and mediated anodic oxidation of organic pollutants, Chem.

395   Rev. 109 (2009) 6541-6569.

396 [7] Y. Zhang, X. Xiong, Y. Han, X. Zhang, F. Shen, S. Deng, H. Xiao, X. Yang, G. Yang, H.

397   Peng, Photoelectrocatalytic degradation of recalcitrant organic pollutants using TiO_2 film

398   electrodes: An overview, Chemosphere 88 (2012) 145-154.

399 [8] W. Wu, Z.-H. Huang, T.-T. Lim, Recent development of mixed metal oxide anodes for

400   electrochemical oxidation of organic pollutants in water, Appl. Catal. A: Gen. 480 (2014) 58-

401   78.

402 [9] C. Comninellis, G.P. Vercesi, Characterization of DSA®-type oxygen evolving electrodes:

403   Choice of a coating, J. Appl. Electrochem. 21 (1991) 335-345.

404 [10] D. Rosestolato, S. Neodo, S. Ferro, G. Battaglin, V. Rigato, A. De Battisti, A comparison

405   between structural and electrochemical properties of iridium oxide-based electrocatalysts

406   prepared by sol-gel and reactive sputtering deposition, J. Electrochem. Soc. 161 (2014) E151-

407   E158.

408 [11] G. Fóti, D. Gandini, C. Comninellis, A. Perret, W. Haenni, Oxidation of organics by
409 intermediates of water discharge on IrO_2 and synthetic diamond anodes, Electrochem. Solid
410 State Lett. 2 (1999) 228-230.

411 [12] S. Aquino Neto, A.R. de Andrade, Electrooxidation of glyphosate herbicide at different DSA[®]
412 compositions: pH, concentration and supporting electrolyte effect, Electrochim. Acta 54
413 (2009) 2039-2045.

414 [13] O. Scialdone, S. Randazzo, A. Galia, G. Filardo, Electrochemical oxidation of organics at
415 metal oxide electrodes: The incineration of oxalic acid at IrO_2-Ta_2O_5 (DSA-O_2) anode,
416 Electrochim. Acta 54 (2009) 1210-1217.

417 [14] O. Scialdone, A. Galia, S. Randazzo, Oxidation of carboxylic acids in water at IrO_2-Ta_2O_5
418 and boron doped diamond anodes, Chem. Eng. J. 174 (2011) 266-274.

419 [15] M. Pérez-Corona, A. Corona, E.D. Beltrán, J. Cárdenas, E. Bustos, Evaluation of IrO_2-
420 Ta_2O_5|Ti electrodes employed during the electroremediation of hydrocarbon-contaminated
421 soil, Sustain. Environ. Res. 23 (2013) 279-284.

422 [16] B. Borbón, M.T. Oropeza-Guzman, E. Brillas, I. Sirés, Sequential electrochemical treatment
423 of dairy wastewater using aluminum and DSA-type anodes, Environ. Sci. Pollut. Res. 21
424 (2014) 8573-8584.

425 [17] E. Mousset, N. Oturan, E.D. van Hullebusch, G. Guibaud, G. Esposito, M.A. Oturan,
426 Treatment of synthetic soil washing solutions containing phenanthrene and cyclodextrin by
427 electro-oxidation. Influence of anode materials on toxicity removal and biodegradability
428 enhancement, Appl. Catal. B: Environ. 160-161 (2014) 666-675.

429 [18] A. Galia, S. Lanzalaco, M.A. Sabatino, C. Dispenza, O. Scialdone, I. Sirés, Crosslinking of
430 poly(vinylpyrrolidone) activated by electrogenerated hydroxyl radicals: A first step towards a
431 simple and cheap synthetic route of nanogel vectors, Electrochem. Commun. 62 (2016) 64-68.

432 [19] M.J.R. Santos, M.C. Medeiros, T.M.B.F. Oliveira, C.C.O. Morais, S.E. Mazzetto, C.A.

433   Martínez-Huitle, S.S.L. Castro, Electrooxidation of cardanol on mixed metal oxide (RuO_2-

434   TiO_2 and IrO_2-RuO_2-TiO_2) coated titanium anodes: insights into recalcitrant phenolic

435   compounds, Electrochim. Acta 212 (2016) 95-101.

436 [20] J.R. Steter, E. Brillas, I. Sirés, On the selection of the anode material for the electrochemical

437   removal of methylparaben from different aqueous media, Electrochim. Acta 222 (2016) 1464-

438   1474.

439 [21] D.T. Araújo, M.A. Gomes, R.S. Silva, C.C. de Almeida, C.A. Martínez-Huitle, K.I.B.

440   Eguiluz, G.R. Salazar-Banda, Ternary dimensionally stable anodes composed of RuO_2 and

441   IrO_2 with CeO_2, SnO_2, or Sb_2O_3 for efficient naphthalene and benzene electrochemical

442   removal, J. Appl. Electrochem. 47 (2017) 547-561.

443 [22] S. Neodo, D. Rosestolato, S. Ferro, A. De Battisti, On the electrolysis of dilute chloride

444   solutions: Influence of the electrode material on Faradaic efficiency for active chlorine,

445   chlorate and perchlorate, Electrochim. Acta 80 (2012) 282-291.

446 [23] O. Scialdone, E. Corrado, A. Galia, I. Sirés, Electrochemical processes in macro and

447   microfluidic cells for the abatement of chloracetic acid from water, Electrochim. Acta 132

448   (2014) 15-24.

449 [24] F. Sopaj, N. Oturan, J. Pinson, F. Podvorica, M.A. Oturan, Effect of the anode materials on

450   the efficiency of the electro-Fenton process for the mineralization of the antibiotic

451   sulfamethazine, Appl. Catal. B: Environ. 199 (2016) 331-341.

452 [25] S. Ellouze, S. Kessemtini, D. Clematis, G. Cerisola, M. Panizza, S.C. Elaoud, Application of

453   Doehlert design to the electro-Fenton treatment of Bismarck Brown Y, J. Electroanal. Chem.

454   799 (2017) 34-39.

455 [26] S. Lanzalaco, I. Sirés, M.A. Sabatino, C. Dispenza, O. Scialdone, A. Galia, Synthesis of

456   polymer nanogels by electro-Fenton process: investigation of the effect of main operation

457   parameters, Electrochim. Acta 246 (2017) 812-822.

458 [27] Y.-U. Shin, H.-Y. Yoo, S. Kim, K.-M. Chung, Y.-G. Park, K.-H. Hwang, S.W. Hong, H.

459   Park, K. Cho, J. Lee, Sequential combination of electro-Fenton and electrochemical

460   chlorination processes for the treatment of anaerobically-digested food wastewater, Environ.

461   Sci. Technol. 51 (2017) 10700-10710.

462 [28] Z.G. Aguilar, E. Brillas, M. Salazar, J.L. Nava, I. Sirés, Evidence of Fenton-like reaction with

463   active chlorine during the electrocatalytic oxidation of Acid Yellow 36 azo dye with Ir-Sn-Sb

464   oxide anode in the presence of iron ion, Appl. Catal. B: Environ. 206 (2017) 44-52.

465 [29] G. Coria, I. Sirés, E. Brillas, J.L. Nava, Influence of the anode material on the degradation of

466   naproxen by Fenton-based electrochemical processes, Chem. Eng. J. 304 (2016) 817-825.

467 [30] S. Trasatti, Electrocatalysis: understanding the success of DSA$^{®}$, Electrochim. Acta 45 (2000)

468   2377-2385.

469 [31] L. Xu, Y. Xin, J. Wang, A comparative study on IrO_2-Ta_2O_5 coated titanium electrodes

470   prepared with different methods, Electrochim. Acta 54 (2009) 1820-1825.

471 [32] X. Qin, F. Gao, G. Chen, Effects of the geometry and operating temperature on the stability of

472   Ti/IrO_2–SnO_2–Sb_2O_5 electrodes for O_2 evolution, J. Appl. Electrochem. 40 (2010) 1797-1805.

473 [33] S. Ferro, D. Rosestolato, C.A. Martínez-Huitle, A. De Battisti, On the oxygen evolution

474   reaction at IrO_2-SnO_2 mixed-oxide electrodes, Electrochim. Acta 146 (2014) 257-261.

475 [34] J.-Y. Lee, An investigation on the electrochemical characteristics of Ta_2O_5-IrO_2 anodes for

476   the application of electrolysis process, Mater. Sci. Appl. 2 (2011) 237-243.

477 [35] E. Lichtfouse, J. Schwarzbauer, D. Robert (Eds.), Environmental chemistry for a sustainable

478   world – Vol. 2: Remediation of air and water pollution, Springer, The Netherlands, 2012.

479   [36] F. Fatone, S. Di Fabio, D. Bolzonella, F. Cecchi, Fate of aromatic hydrocarbons in Italian

480   municipal wastewater systems: an overview of wastewater treatment using conventional

481   activated-sludge processes (CASP) and membrane bioreactors (MBRs), Water Res. 45 (2011)

482   93-104.

483   [37] W. Wang, J. Wang, Different partition of polycyclic aromatic hydrocarbon on environmental

484   particulates in wastewater: Microplastics in comparison to natural sediment, Ecotoxicol.

485   Environ. Safety 147 (2018) 648-655.

486   [38] O.M. Lönnstedt, P. Eklöv, Environmentally relevant concentrations of microplastic particles

487   influence larval fish ecology, Science 352 (2016) 1213-1216.

488   [39] Directive 2000/60/EC of the European Parliament and of the Council establishing a

489   framework for Community action in the field of water policy official J. L 327, 22 December

490   2000, pp. 0001–0073 (www.europa.eu.int.).

491   [40] D. Han, M.J. Currell, Persistent organic pollutants in China's surface water systems, Sci. Total

492   Environ. 580 (2017) 602-625.

493   [41] J. Muff, E.G. Søgaard, Electrochemical degradation of PAH compounds in process water: a

494   kinetic study on model solutions and a proof of concept study on runoff water from harbour

495   sediment purification, Water Sci. Technol. 61 (2010) 2043-2051.

496   [42] A. Yaqub, M.H. Isa, H. Ajab, Electrochemical degradation of polycyclic aromatic

497   hydrocarbons in synthetic solution and produced water using a Ti/SnO_2-Sb_2O_5-RuO_2 anode, J.

498   Environ. Eng. 141 (2015) 1-8.

499   [43] E. Pepprah, M.V. Khire, Electroremediation of naphthalene in aqueous solution using

500   alternating and direct currents, J. Environ. Eng. 134 (2008) 32-41.

501   [44] R.A. Herrada, A. Medel, F. Manríquez, I. Sirés, E. Bustos, Preparation of IrO_2-Ta_2O_5|Ti

502   electrodes by immersion, painting and electrophoretic deposition for the electrochemical

503   removal of hydrocarbons from water, J. Hazard. Mater. 319 (2016) 102-110.

504 [45] D. Rosestolato, S. Neodo, S. Ferro, G. Battaglin, V. Rigato, A. De Battisti, A comparison

505 between structural and electrochemical properties of iridium oxide-based electrocatalysts

506 prepared by sol-gel and reactive sputtering deposition, J. Electrochem. Soc. 161 (2014) E151-

507 E158.

508 [46] G. Battaglin, D. Rosestolato, S. Ferro, A. De Battisti, Characterization of IrO_2-SnO_2 films

509 prepared by physical vapor deposition at ambient temperature, Electrocatalysis 4 (2013) 358-

510 366.

511 [47] S. Fierro, A. Kapałka, C. Comninellis, Electrochemical comparison between IrO_2 prepared by

512 thermal treatment of iridium metal and IrO_2 prepared by thermal decomposition of H_2IrCl_6

513 solution, Electrochem. Commun. 12 (2010) 172-174.

514 [48] NACE International, Standard test method TM0108 Testing of Catalyzed Titanium Anodes

515 for Use in Soils or Natural Waters, 2012.

516 [49] T. Maezono, M. Tokumura, M. Sekine, Y. Kawase, Hydroxyl radical concentration profile in

517 photo-Fenton oxidation process: Generation and consumption of hydroxyl radicals during the

518 discoloration of azo-dye Orange II, Chemosphere 82 (2011) 1422-1430.

519 [50] C.A. Huang, S.W. Yang, C.Z. Chen, F.-Y. Hsu, Electrochemical behavior of IrO_2-Ta_2O_5|Ti

520 anodes prepared with different surface pretreatments of Ti substrate, Surf. Coat. Technol. 320

521 (2017) 270-278.

522 [51] M.R. Heinrich, A. Gansäuer (Eds.), Radicals in Synthesis III, Topics in Current Chemistry,

523 Book 320, Springer-Verlag, Heidelberg, 2012.

524 [52] C.A. Paddon, C.E. Banks, I.G. Davies, R.G. Compton, Oxidation of anthracene on platinum

525 macro- and micro-electrodes: Sonoelectrochemical, cryoelectrochemical and

526 sonocryoelectrochemical studies, Ultrason. Sonochem. 13 (2006) 126-132.

527

528 **Figure captions**

529 **Figure 1**. Scanning electron micrographs of the surfaces of the IrO_2-Ta_2O_5|Ti electrodes

530 manufactured by electrodeposition, using four different Ir:Ta molar ratios, followed by thermal

531 decomposition. Magnification: (A) 2000x and (B) 5000x.

532 **Figure 2**. Atomic percentages of Ti, Ir, Ta and oxygen analyzed by EDX for the four IrO_2-Ta_2O_5|Ti

533 electrodes manufactured with different Ir:Ta molar ratios as seen on the x axis.

534 **Figure 3**. Cyclic voltammograms recorded using each of the four IrO_2-Ta_2O_5|Ti materials (0.75 cm^2

535 of exposed surface area), with different Ir:Ta molar ratios, as the working electrode in 0.5 M H_2SO_4

536 at room temperature. Counter electrode: Pt wire. Reference electrode: Ag|AgCl (3 M KCl). Scan

537 rate: 50 mV s^{-1}.

538 **Figure 4.** UV/vis spectra of 10 mL of a 0.3 mM coumarin solution in 0.5 M H_2SO_4, electrolyzed for

539 180 min at 50 mA and room temperature under constant stirring. Each single IrO_2-Ta_2O_5|Ti

540 electrode (0.75 cm^2) at a given Ir:Ta molar ratio and a Pt wire were employed as the anode and

541 cathode, respectively. The spectrum of coumarin at time zero is also shown for reference.

542 **Figure 5**. 7-Hydroxycoumarin concentration accumulated over time during the experiments

543 described in Fig. 4. Data were obtained from an HPLC instrument coupled to a fluorescence

544 detector.

545 **Figure 6**. (A) Decay of phenanthrene concentration with electrolysis time during the electro-

546 oxidation of 50 mL of solutions containing ~ 2 μM of the hydrocarbon in 0.05 M Na_2SO_4 at natural

547 pH and room temperature by applying 50 mA. Each IrO_2-Ta_2O_5|Ti electrode (0.75 cm^2) at given

548 Ir:Ta molar ratios and a Pt plate were employed as the anode and cathode, respectively. (B) Decay

549 of naphthalene during analogous treatments. The horizontal dashed lines represent the limit of

550 quantification for both PAHs under the selected analytical conditions.

23

551 **Figure 7**. (A) TOC abatement vs time during the electro-oxidation of 50 mL of a 25 mg·L^{-1} (0.19

552 mM) naphthalene solution in 0.05 M Na$_2$SO$_4$ at natural pH and room temperature by applying 50

553 mA. Each single IrO$_2$-Ta$_2$O$_5$|Ti electrode (0.75 cm^2) at a given Ir:Ta molar ratio and a Pt plate were

554 employed as the anode and cathode, respectively. (B) Mineralization current efficiency calculated

555 from Eq. (4) for the above trials.

556 **Figure 8**. Service life of each manufactured electrode, at a given Ir:Ta molar ratio, determined

557 according to NACE TM0108 standard procedure.

24

Figure 1

(A)   **(B)**
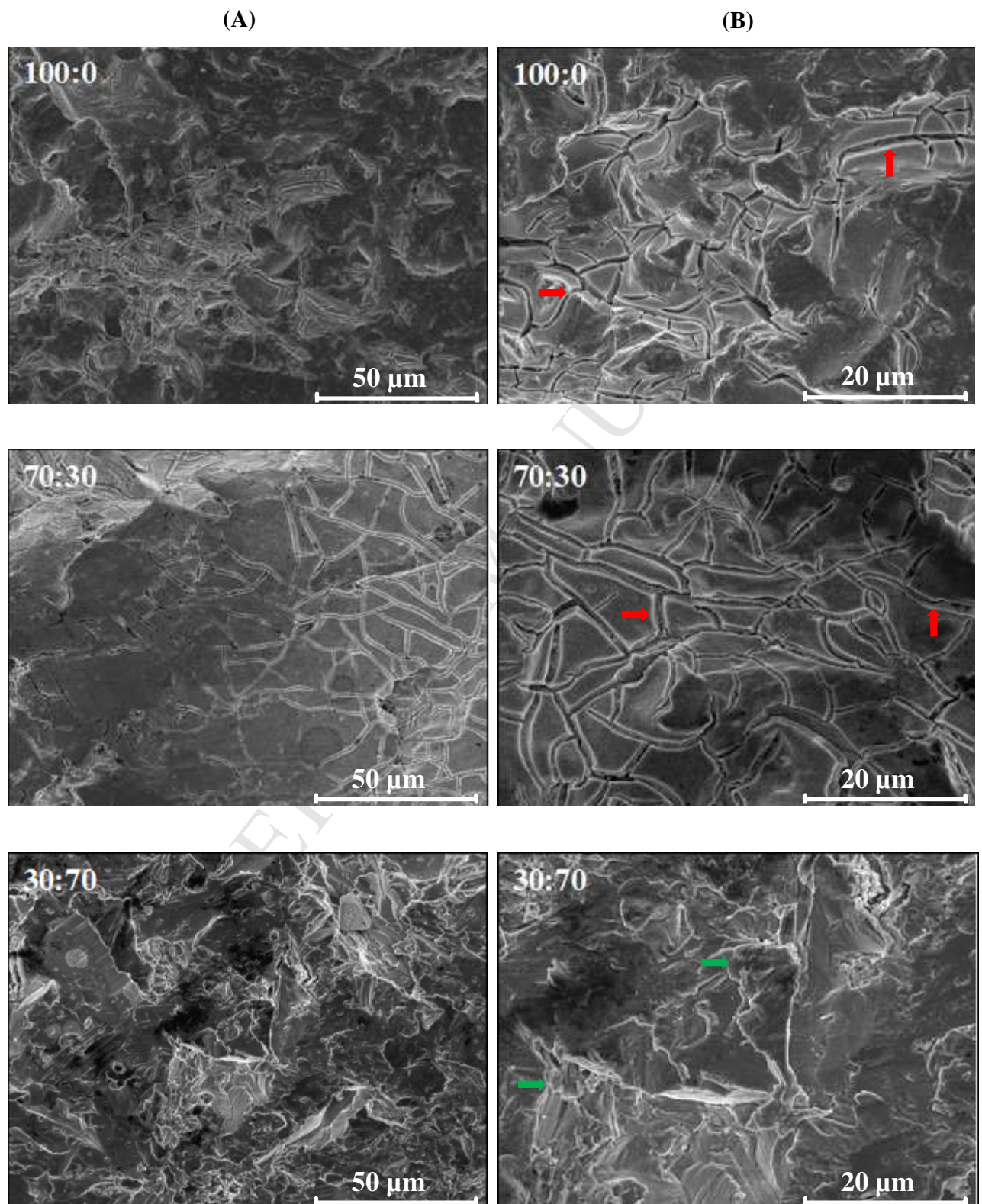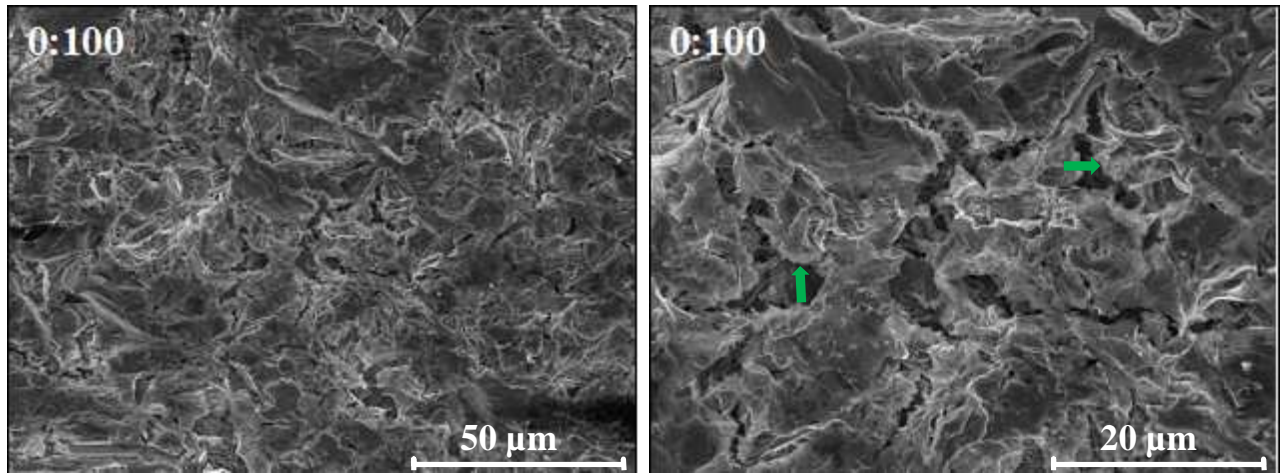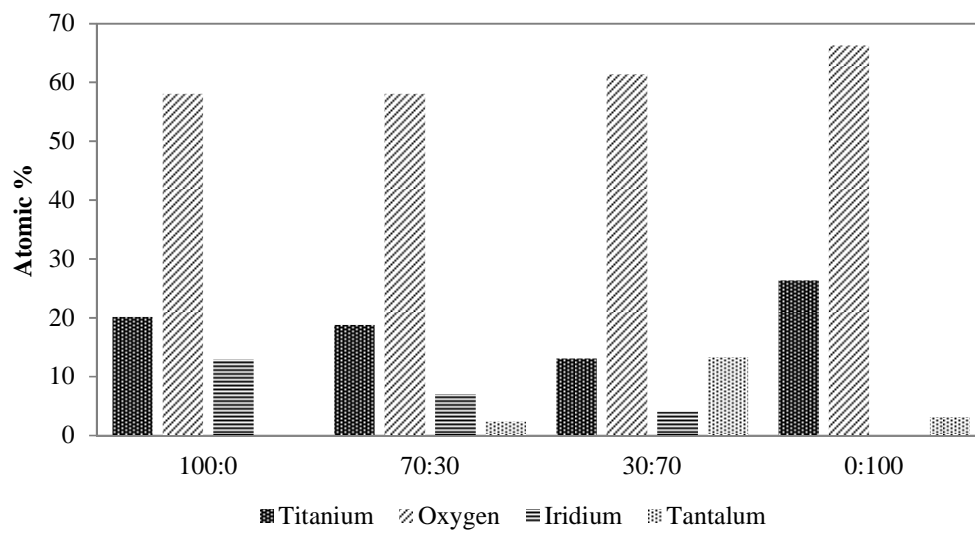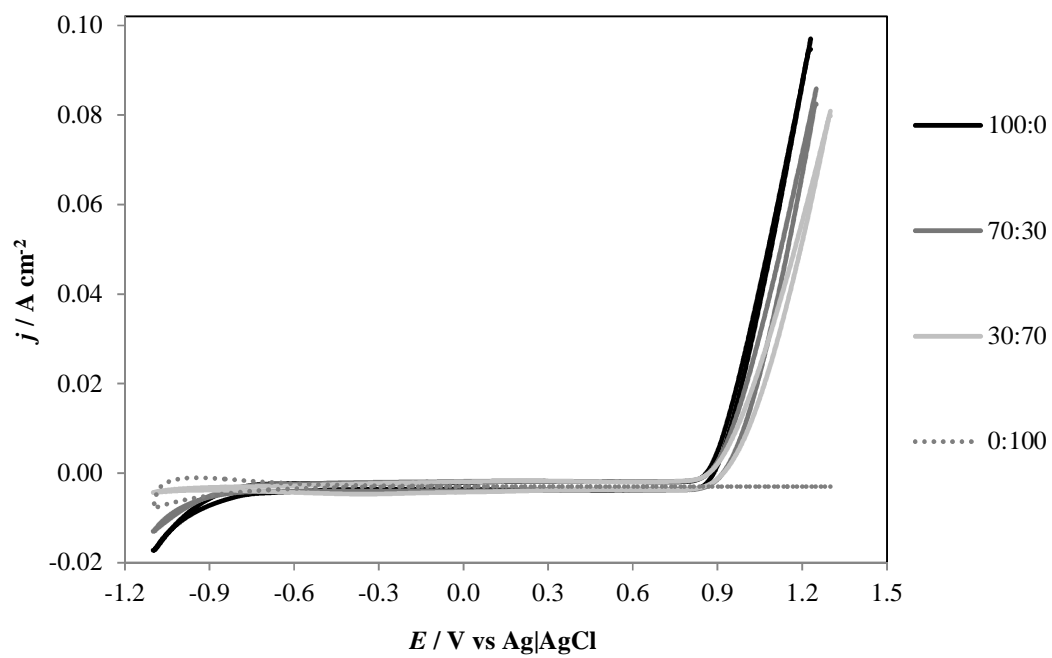
Figure 2

Figure 3

Figure 4
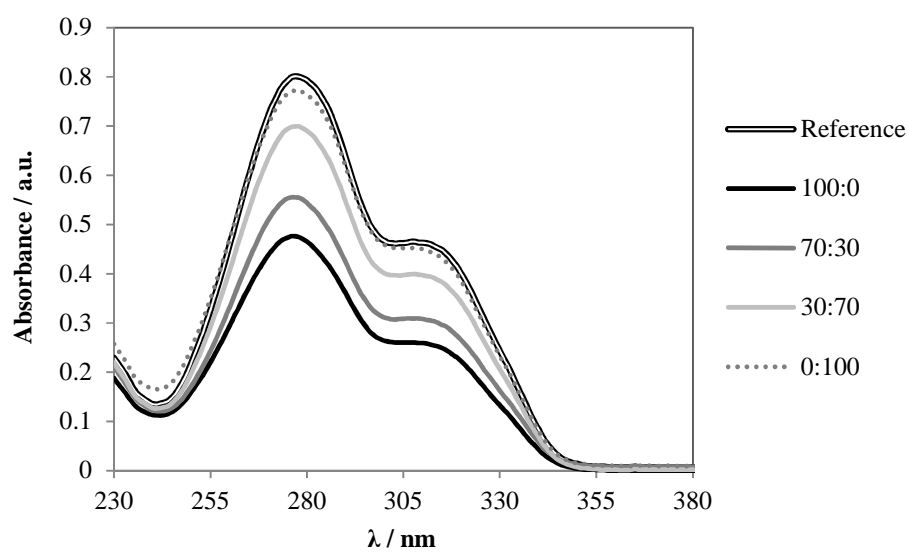
Figure 5
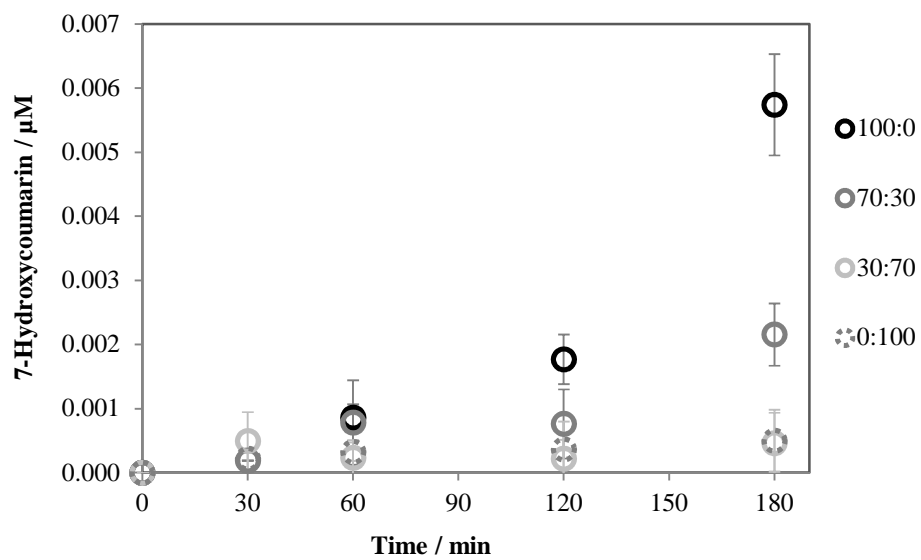
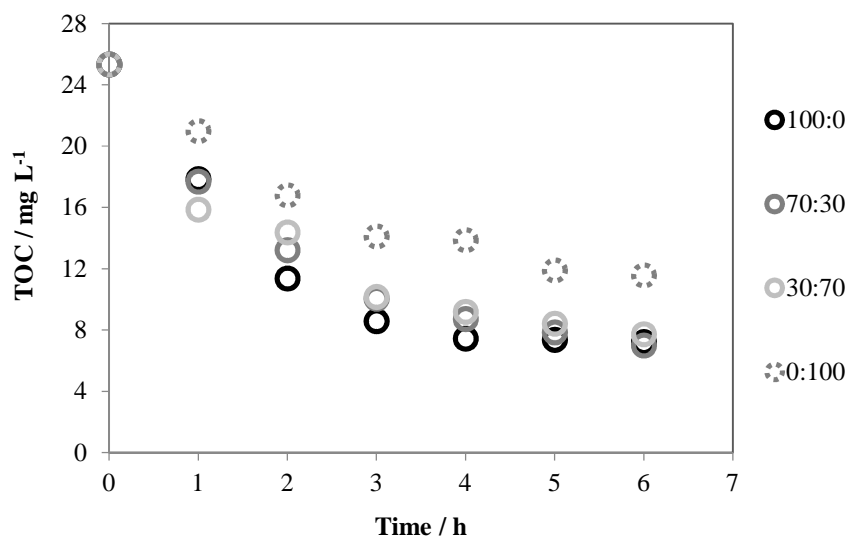**Figure 6**

(A)
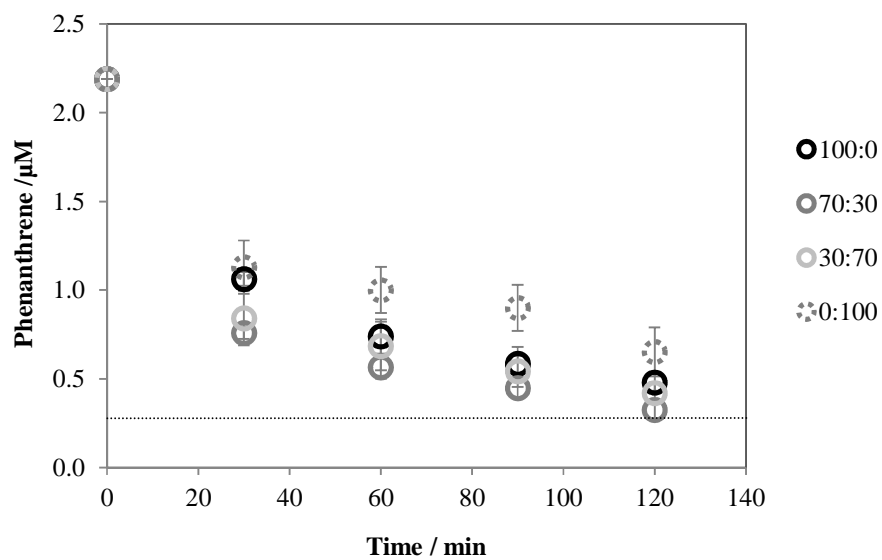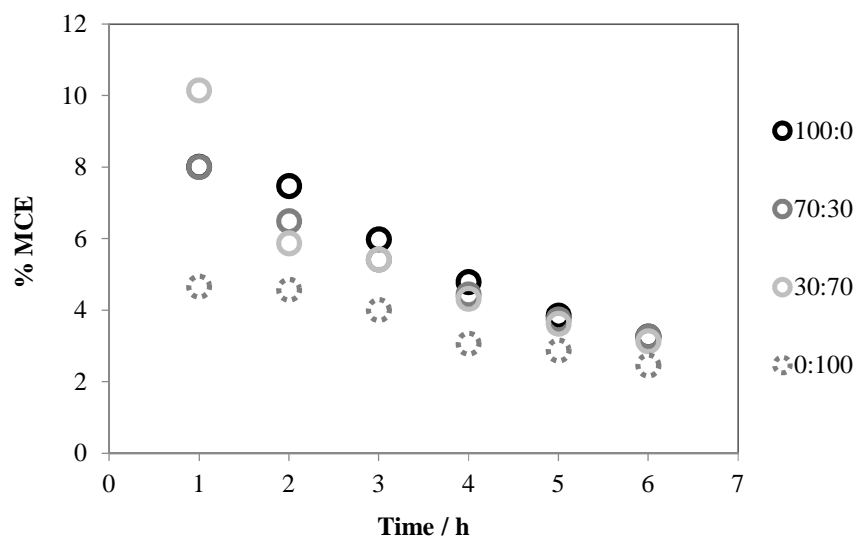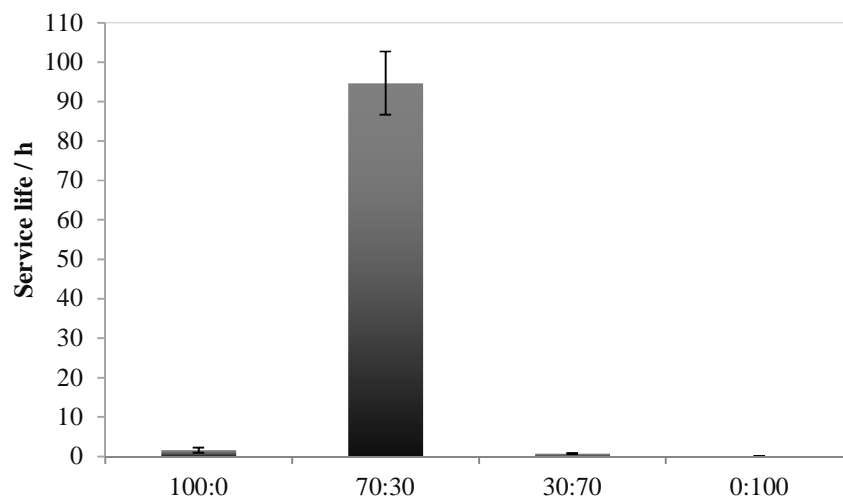

(B)
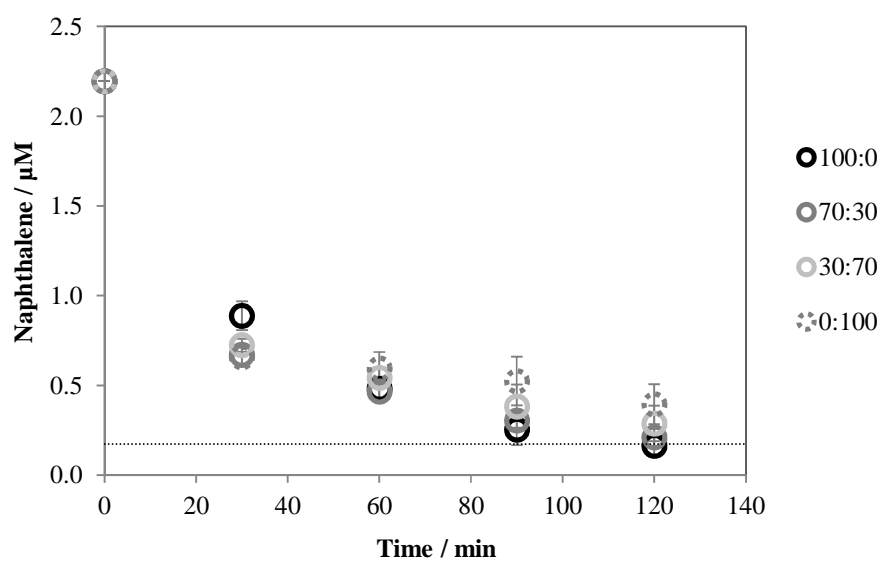
Figure 7

(A)

(B)

Figure 8

Highlights

- High quality coatings by electrodeposition followed by thermal treatment: 70% or 100% Ir

- Production of M($^\bullet$OH) clearly increased in the order (Ir:Ta): 0:100 < 30:70 < 70:30 < 100:0

- Electro-oxidation of PAHs using IrO_2-Ta_2O_5|Ti anodes: direct + M($^\bullet$OH)-mediated oxidation

- Up to 86% and 93% removal of phenanthrene and naphthalene, along with 74% TOC abatement

- IrO_2-Ta_2O_5|Ti electrode with Ir:Ta 70:30 showed highest electrocatalytic power and service life